Dynamics of solitary waves in smectic-C^* liquid crystals

E. N. Tsoy,[1] I. W. Stewart,[2] and F. Kh. Abdullaev[1]
[1]*Physical-Technical Institute of the Uzbek Academy of Sciences, Mavlyanova str., 2-b, Tashkent 700084, Uzbekistan*
[2]*Department of Mathematics, Strathclyde University, Glasgow G1 1XH, Scotland, United Kingdom*
(Received 26 October 1998)

The dynamics of solitary waves in ferroelectric liquid crystals is considered in the context of an overdamped double sine-Gordon model. Various possible types of single waves are studied. The dependence of wave velocity and scale on the system parameters and initial conditions is found. Sharp initial profiles lead to waves with a universal form. The parameters of the wave arising from smooth profiles are determined also by the scale of the initial conditions. Numerical calculations show good agreement with analytical results. The possibility of using such waves to improve the characteristics of liquid crystal devices is also discussed. [S1063-651X(99)10810-9]

PACS number(s): 61.30.Gd, 05.45.Yv

I. INTRODUCTION

Static and dynamic structures in liquid crystals, forming because of inhomogeneity in space and the time-dependent distribution of the average molecular orientation, are the focus of intensive research [1–3]. The study of such structures is useful both for determining liquid crystal properties and as a basis of new electro-optical devices. The average local molecular orientation is described by the unit vector **n**, called the director. In many cases solitary waves occur (''walls,'' ''fronts,'' or ''kinks'') that propagate from a region with stable molecular orientation into an unstable or metastable region. Often, such a wave has an asymptotically universal form and velocity, not dependent upon the peculiarities of the initial conditions. In such cases the corresponding equation for the director motion is frequently a type of nonlinear diffusion equation that exhibits such phenomena. Different processes in liquid crystals are described by this approach: orientational waves in nematics under magnetic or electric fields, cholesteric-nematic transitions induced by a magnetic field, walls in electro-hydrodynamic instabilities in liquid crystals, switching in smectic liquid crystals, etc. (see Refs. [2,4], and the references therein).

The reorientation of molecules in ferroelectric smectic-C^* liquid crystals (FLCs) through a propagation of solitary waves (''domain walls'') was first investigated by Cladis *et al.* [5]. They analyzed the driven sine-Gordon equation by taking into account the inertia term. It is known that the influence of this term is negligible in many types of liquid crystals [1]. The model, based on a nonlinear diffusion equation, for solitary waves in FLCs was first suggested by Maclennan *et al.* [6]. Further studies can be found in the review [7], where methods of analysis, theoretical results, and numerical calculations of FLC dynamics are presented. In this review both the cases of thick and thin liquid crystal samples are considered. The latter case is characterized by a strong influence of the boundaries upon the sample alignment; that is, the surface alignment of the glass plates bounding the sample cell affect the bulk behavior. Interesting experiments and numerical simulations for thin FLC cells are presented in [8]. Results, based on a ''marginal stability'' theory, for the velocity of solitary waves in smectic-C^* samples are described in [9].

In the present paper some parameters of solitary waves, such as the velocity and the width, in FLCs are determined. The analytical dependence of parameters on the amplitude of the electric field and properties of the liquid crystal is found. A choice of appropriate boundary conditions is shown to increase the velocity of waves. Using such a possibility, one can decrease the switching time of liquid crystal electro-optical devices. The paper is organized as follows. In Sec. II the model for describing FLC dynamics, based on an overdamped double sine-Gordon (DSG) equation, is presented. We describe also a simple procedure for determining the wave velocity. Possible types of solitary waves in smectic-C^* samples and the dependence of the velocity on the system parameters are considered in Sec. III. The influence of various boundary conditions and the evolution of solutions from two-kink initial conditions are also discussed. Section IV briefly summarizes the results obtained.

II. MODEL AND METHOD OF ANALYSIS

Smectic-C^* liquid crystals are layered structures in which the director **n** has the constant tilt angle θ with respect to the layer normal. The azimuthal angle of the director changes gradually from layer to layer, forming the well known helical structure [1]. This description is valid for large infinite samples. We study thin or ''surface stabilized'' FLC cells [10], with thickness d of order less than the helical pitch, and suppose that the smectic layers are oriented parallel to the xy plane. The influence of plate boundary surfaces in such cells is strong enough to suppress the helix, so that the director distribution is uniform in the z direction and changes only in the x direction (Fig. 1). The polarization **p** is normal to **n** and the z axis. Let ϕ be the azimuthal angle of **p**, i.e., $\phi=\pi/2-\psi$, where ψ is the orientation angle of the orthogonal projection of **n** onto the smectic layers. Assuming that the smectic tilt angle θ is constant, the equation for the director motion has the form [7,11]

$$\eta\phi_t - K\phi_{xx} = -PE\sin\phi + \frac{\epsilon_a E^2 \sin^2\theta}{4\pi}\sin\phi\cos\phi, \quad (1)$$

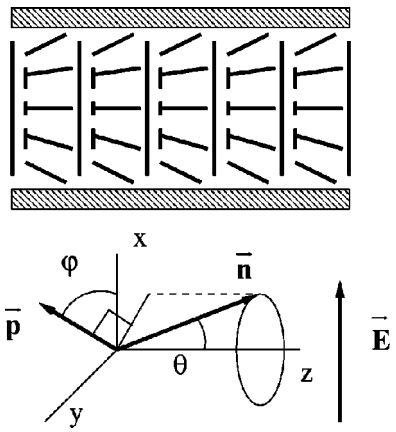

FIG. 1. Director distribution in a thin ''surface stabilized'' FLC cell. ''Nails'' mean molecules are directed out of the figure plane.

where η is a viscosity coefficient, K is an elastic constant, E is the magnitude of the electric field applied in the plane of smectic layers parallel to the x axis, and ϵ_a is the dielectric anisotropy. In the notation of the smectic continuum theory of Leslie *et al.* [12,13], η is equal to the rotational viscosity coefficient λ_5 of the director around a fictitious ''cone,'' while $K=B_3$. The first term on the right-hand side of Eq. (1) is the ferroelectric torque and the second term is the dielectric torque. Boundary conditions ought to be chosen so that $\phi(x=-d/2,t)=\phi_L$ and $\phi(x=d/2,t)=\phi_R$ where ϕ_L and ϕ_R are constants. Nevertheless, to enable a more tractable investigation that exhibits the qualitative features and the general properties of solitary waves in the above system, we consider the case as $d\to\infty$. Consequently, we consider the case of an infinite system.

In dimensionless variables, Eq. (1) has the form [7]

$$\phi_\tau-\phi_{\xi\xi}+\sigma\sin\phi+a\sin(2\phi)=0, \tag{2}$$

where $\xi=x/x_0$ $x_0=[K/(|PE|)]^{1/2}$, $\tau=t/t_0$, $t_0=\eta/(|PE|)$, $\sigma=\mathrm{sgn}(E)$, $a=-\epsilon_a\sigma E\sin^2\theta/(8\pi P)$. Since Eq. (2) is invariant with respect to the transformation $\sigma\to-\sigma,\phi\to\pi-\phi$ or $\phi\to\pi+\phi$, we consider only the case $\sigma=1$. Equation (2) is the overdamped double sine-Gordon equation, which can also describe the dynamics of smectic-C liquid crystals subjected to electric fields that are tilted with respect to the smectic planes [14,15]. Equation (2) is a type of nonlinear diffusion equation for which it is known that solitary waves arising from a wide class of initial conditions have a universal form and velocity [4,16,17].

Let us describe the procedure for finding asymptotic values as $\tau\to\infty$ for the wave parameters in the nonlinear diffusion equation of the form

$$\phi_\tau-\phi_{\xi\xi}+F(\phi)=0, \tag{3}$$

where $F(\phi)$ is some nonlinear function. Boundary conditions are of the first or the second kind ($\phi_\xi=0$ at $\xi=\pm\infty$) and initial conditions are assumed to be piecewise continuous. The procedure below is some combination of phase plane analysis (see, e.g., [4,16,17]), ''marginal stability'' theory [19,20], and Hagan's theory [18]. We believe that this procedure is one of the simplest ways to obtain complete and exact information about solitary waves. Phase plane analysis gives all possible types of waves, while the two other theories allow us to find wave parameters. The approach can be called ''the principle of the least dissipation.'' It means that the velocity of the steady state wave of Eq. (3) is equal to the *lowest* possible dissipation on the trajectory of the corresponding ordinary differential equation [see Eq. (4)]. The trajectory should satisfy appropriate boundary and other conditions. Thus, instead of dealing with the dispersion relation of the linearized version of Eq. (3) as it is in ''marginal stability theory,'' one can analyze Eq. (4).

Step (i). Since we are interested in stationary solutions, it is reasonable to reduce Eq. (3) to an ordinary differential equation by introducing the usual variable $X=\xi-v\tau$, where v is the wave velocity. This yields the equation

$$\frac{d^2\phi}{dX^2}+v\frac{d\phi}{dX}+\frac{dV(\phi)}{d\phi}=0,\quad F(\phi)\equiv-\frac{dV(\phi)}{d\phi}. \tag{4}$$

Equation (4) is the equation of motion of a particle in a potential $V(\phi)$ in the presence of ''dissipation'' with coefficient v.

Step (ii). Find equilibrium points ϕ_e of Eq. (4) or static uniform states of Eq. (3) from the condition $dV(\phi)/d\phi=0$. Check the stability of these equilibrium points by calculating $V''(\phi_e)\equiv d^2V(\phi_e)/d\phi^2$. If $V''(\phi_e)<0$ [$V''(\phi_e)>0$], the point ϕ_e is stable (unstable). Determine the type of equilibrium points in the phase plane by finding characteristic exponents λ ($\phi=\phi_e+\delta\phi e^{-\lambda X}$):

$$\lambda_\pm(v,\phi_e)=\frac{v\pm\sqrt{v^2-4V''(\phi_e)}}{2}. \tag{5}$$

If $\lambda_\pm$ are complex with $\mathrm{Im}(\lambda_\pm)\neq0$, then ϕ_e is a focus. If $\lambda_\pm$ are real and $\lambda_+\lambda_-<0$ then ϕ_e is a saddle (S), while if $\lambda_\pm$ are real and $\lambda_+\lambda_->0$, then ϕ_e is a node (N). Note that stable (unstable) points of Eq. (4) or minima (maxima) of $V(\phi)$ correspond to unstable (stable) static states of Eq. (3) (see also the paper by Lam in Ref. [2] and review [7]).

Step (iii). Construct possible types of solitary waves. Hereafter we assume that $\phi(-\infty,\tau)=\phi_L$ and $\phi(\infty,\tau)=\phi_R$, where ϕ_L,ϕ_R are static states. Hence the solitary wave is a front moving from a stable state to an unstable (metastable) state. In order to simplify this step of the procedure it is easiest to plot the phase plane consisting of ϕ and $d\phi/dX$ for Eq. (4). The phase trajectory, connecting two given equilibrium points ϕ_L and ϕ_R, then corresponds to a solitary wave. As a result of the boundary conditions for Eq. (3), any equilibrium point cannot be a focus; this indicates that only the following types of solitary waves are possible: $[N-N]$, $[N-S]$ or $[S-N]$ and $[S-S]$. Here, the notation $[A-B]$ indicates a front moving from A to B as $X\to\infty$.

Step (iv). Find the asymptotic velocity as $\tau\to\infty$ and the width of each solitary wave. An $[N-N]$ wave is usually a collection of two or more waves, and it should be considered separately (see Sec. III). In most cases (see [4,17,18]), the velocity of $[S-S]$ waves is definite; i.e., the phase trajectory, connecting two saddle points, exists only for a unique value of the ''dissipation'' $v=v_s$. This means that any initial condition with boundary conditions, corresponding to saddle points, tends to a solitary wave moving with speed v_s. Another situation is the case of solitary waves with a

TABLE I. Types of solitary waves.

Parameter a ($\sigma=1$)	Wave type	Asymptotic states	Wave velocity for initial conditions: Sharp	Smooth
$a<-1/2$	$[S-S]$	$[\phi_N \leftrightarrow (2\pi-\phi_N)]$	0	0
	$[S-N]$	$[\phi_N \rightarrow 0]$	v_1	$v_{1\beta}$
	$[S-N]$	$[\phi_N \rightarrow \pi]$	v_3	$v_{3\beta}$
	$[S-N]$	$[(2\pi-\phi_N) \rightarrow \pi]$	v_3	$v_{3\beta}$
$\lvert a\rvert<1/2$	$[S-S]$	$[0 \leftrightarrow 2\pi]$	0	0
	$[S-N]$	$[0 \rightarrow \pi]$	$\geqslant v_3$	$v_{3\beta}$
$a>1/2$	$[S-S]$	$[0 \leftrightarrow 2\pi]$	0	0
	$[S-N]$	$[0 \rightarrow \phi_N]$	$\geqslant v_2$	$v_{2\beta}$
	$[S-N]$	$[\pi \rightarrow \phi_N]$	v_2	$v_{2\beta}$
	$[S-N]$	$[\pi \rightarrow (2\pi-\phi_N)]$	v_2	$v_{2\beta}$
	$[S-S]$	$[0 \rightarrow \pi]$	v_4	v_4

node as one of the asymptotic states. As for any equilibrium point, a node is characterized by two eigenvalues [see Eq. (5)]. The greater in absolute value is called ''usual'' and one says that $\phi(\xi,\tau)$ decays in ξ at a usual rate. The other eigenvalue is ''accidental'' and the corresponding rate is called accidental. In the case $v>0$, so that $V(\phi)>0$ and $\lambda_{\pm}>0$, λ_+ is the usual eigenvalue and λ_- is the accidental eigenvalue. These eigenvalues determine space scales, depending on how the evolution of initial conditions changes. Let us assume that the behavior of $\phi(\xi,0)$ at infinity is as follows:

$$\phi(\xi,0)=\phi_L+\delta_1 e^{\beta\xi} \quad \text{as} \quad \xi\rightarrow-\infty, \tag{6}$$

$$\phi(\xi,0)=\phi_R+\delta_2 e^{-\beta\xi} \quad \text{as} \quad \xi\rightarrow\infty, \tag{7}$$

where $\beta>0$. One says the initial condition is ''sharp,'' if $\beta>\lambda_{\text{th}}$ and ''smooth'' when this inequality is reversed, where λ_{th} is the threshold scale. The velocity of sharp initial profiles for solitary $[N-S]$ waves is determined from the condition that ensures that $\lambda_{\pm}$ is real or equivalently $D\equiv v^2-4V''(\phi_N)=0$ where ϕ_N is a node equilibrium; therefore the velocity is given by (see [4,16,17])

$$v^*=\pm 2\sqrt{V''(\phi_N)}. \tag{8}$$

The choice of sign in the above depends on where the node ϕ_N is situated. The threshold scale can be found from the condition

$$\lambda_{\text{th}}=\lvert\lambda\pm(v^*,\phi_N)\rvert=\lvert v^*/2\rvert. \tag{9}$$

The asymptotic velocity for smooth initial profiles is determined from the condition $\lambda_-=\beta$. This means that the behavior of the initial profile as $\xi\rightarrow\pm\infty$ determines the shape of the resulting wave and consequently its velocity. Thus the velocity of a solitary $[N-S]$ wave arising from smooth initial conditions is

$$v^*_\beta=\pm\frac{\beta^2+V''(\phi_N)}{\beta}, \tag{10}$$

where the index β indicates dependence on the initial rate β. Therefore, any sharp initial condition tends to a solitary $[N-S]$ wave with a universal shape and velocity v^*, while a smooth initial profile tends to a solitary wave with its shape and velocity depending on the initial rate β. Details, restrictions for the function $V(\phi)$ and proofs of some related results can be found in [18].

The space scale of the wave, or the width $w_{1/2}$, can be determined as the half-amplitude width of $\phi_\xi(\xi,\tau)$. The width $w_{1/2}$ can be estimated by using characteristic exponents, so that $w_{1/2}\sim 1/\lambda(v,\phi_L)+1/\lambda(v,\phi_R)$, where the appropriate v from Eq. (8) or Eq. (10) should be chosen.

The velocity v^* is the same as that predicted by marginal stability theory [19,20]. It follows from the theory that there exists a threshold velocity, so that fast traveling waves are stable. Due to a ''selection mechanism,'' the asymptotic velocity tends to the threshold value. However, the theory does not consider the dependence of the velocity on the initial conditions for smooth profiles. Notice that Eqs. (8)–(10) are valid under the assumption that the corresponding wave is *monotonic*. Below, we also consider cases where our approach, and that of marginal stability theory, are not applicable. It is shown that marginal stability theory can be extended to incorporate additional conditions. In the case of the overdamped DSG equation the additional condition of monotonicity for the asymptotic profile should be supposed.

III. APPLICATION TO THE OVERDAMPED DSG EQUATION

The reduction of the overdamped DSG equation (2) has the form of Eq. (4) with the potential

$$V(\phi)=-[\sigma(1-\cos\phi)+a(1-\cos(2\phi))/2]. \tag{11}$$

Therefore for any parameter a there exist static states $\phi=\pi k$, where k is an integer; further, for $\lvert a\rvert>1/2$, additional states $\phi_N=\pm\cos^{-1}[-\sigma/(2a)]+2\pi k$ appear in the system. All possible types of solitary waves, corresponding to equilibrium states at $\xi=\pm\infty$ with the appropriate wave velocities, are listed in Table I, where the velocities are calculated using

Eqs. (8) and (10):

$$v_1=\pm\sqrt{-4(\sigma+2a)}, \quad v_{1\beta}=\pm(\beta^2-\sigma-2a)/\beta,$$
$$v_2=\pm\sqrt{2(4a^2-\sigma^2)/a}, \quad v_{2\beta}=\pm\left(\beta^2+\frac{4a^2-\sigma^2}{2a}\right)\Big/\beta, \tag{12}$$
$$v_3=\pm\sqrt{4(\sigma-2a)}, \quad v_{3\beta}=(\beta^2+\sigma-2a)/\beta.$$

The dependence of v_3 (for $\sigma=1$ and $a<0$) on the system parameters was also found by Maclennan *et al.* [7], who applied the result from Ref. [16]. The velocity v_4 corresponds to the exact solution of Eq. (2) found by Schiller *et al.* [14]:

$$\phi(\xi,\tau)=2\tan^{-1}[\exp(\sqrt{2a}(x-v_4t)], \tag{13}$$
$$v_4=[1/(2a)]^{1/2}.$$

The dynamics of solitary waves in FLCs was also considered by van Saarloos *et al.* [9], who studied only the case for $[0\ -\pi]$ waves for different values of fields, while other types of waves were not analyzed. The exact solution, Eq. (13), and other complex solutions to Eq. (1), can be derived via a Painlevé analysis [21]; Stewart [22] has examined the stability of this solution in the context of traveling waves for nonlinear diffusion equations and Cladis and van Saarloos [11] have also discussed marginal stability.

To check the analytical predictions we calculated Eq. (2) numerically for $\sigma=1$ and various values for the parameter a. Both piecewise linear and tanh initial conditions were used. The first type of profile to be considered consists of two uniform states at the ends of the space interval, connected by a linear function. The second type considered is represented by the equation

$$\phi=\phi_L+\frac{\phi_R-\phi_L}{2}(1+\tanh\beta\xi), \tag{14}$$

for some constant β. The calculations were performed using the explicit finite difference method (see, e.g., [23], Chap. 17) with a four-point, two-layer scheme. The space and time steps were equal to 0.05 and 0.0005, respectively, for most calculations. Fixed boundary conditions $\phi(\pm L/2,\tau)=\text{const}$ were used. The parameter σ was set to 1 and the length of the system L was varied from 50 to 100. It should be noted that numerical simulations of Eq. (2) in a wide region of parameters were also performed by Maclennan *et al.* [7]. They have computed director reorientation times as a function of the electric field and system parameters. The authors of paper [7] have also shown that for small L (or for small E), the dynamics are conditioned by transition processes, while for cells with large enough L (or for large E) the dynamics are determined by the evolution of a steady state wave. Our consideration corresponds to the case of large L, when the obtained formulas (12) are valid. An important point is that we also consider various boundary conditions.

In all numerical simulations, after a short transition process, the solitary wave moves with fixed velocity and form (within the accuracy of calculations). The typical evolution for a $[0\to\phi_N]$ wave form is presented in Fig. 2; the dynamics of solitary waves with other boundary conditions is similar. Results, summarized in Figs. 3 and 4, show a good agreement between the two approaches. Figure 3 represents the dependence of the asymptotic velocity on the parameter a for various waves, while Fig. 4 shows the dependence of the asymptotic velocity on the space scale of the initial condition dependent upon β. However, there is a noticeable deviation in the results for $[0\to\phi_N]$ and $[0\to\pi]$ waves, when a is close to 1/2. Numerically obtained velocities exceed the expected theoretical values [see Eq. (12)]. This result can be explained in the following way (we consider for simplicity only a $[0\to\phi_N]$ wave). Indeed, the equilibrium ϕ_N becomes a node at $v=v_2$, but the separatrix $[0-\phi_N]$ also crosses the ϕ axis at some point $\phi_C>\phi_N$ (Fig. 5). The corresponding solitary wave is therefore not monotonic (see the inset in Fig. 5). The monotonic profile will be realized for $v>v_2$, at which the separatrix approaches the point ϕ_N from below.

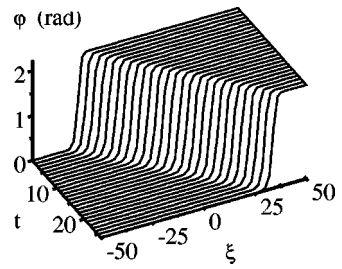

FIG. 2. Typical evolution of the $[0\to\phi_N]$ wave for $a=1$.

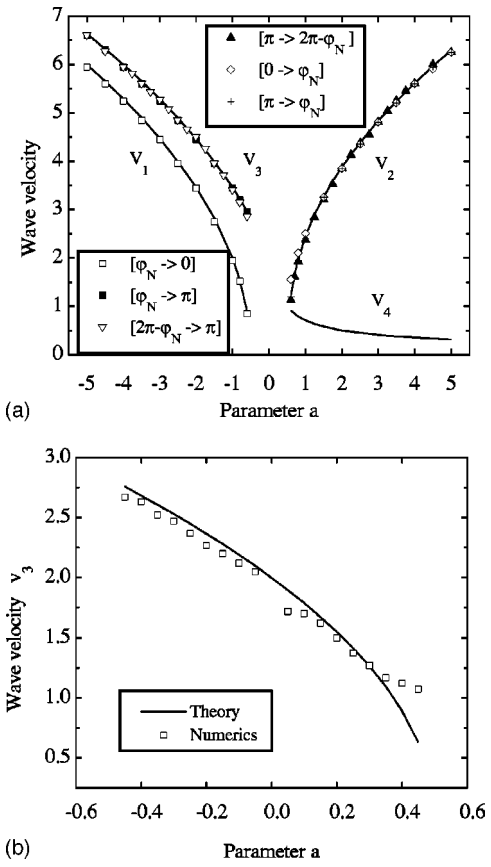

FIG. 3. Comparison of analytical (lines) and numerical (points) results for sharp initial conditions. Corresponding waves are indicated near each type of point. (a) $|a|>1/2$; (b) $|a|<1/2$, $[0\to\pi]$ wave.

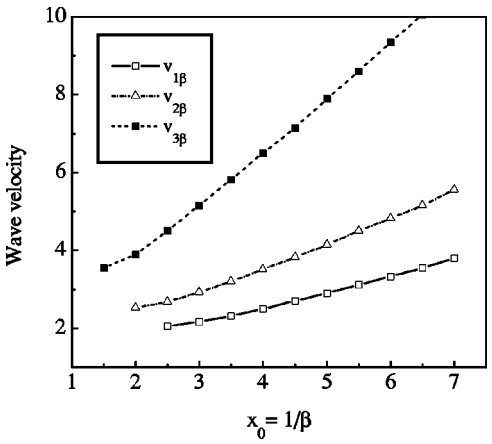

FIG. 4. Dependence of the wave velocity on the initial rate for smooth initial conditions. $a=-1$ for the $[\phi_N \to 0]$ wave with $v_{1\beta}$, $x_{0\mathrm{th}}=2.0$; $a=1$ for the $[0 \to \phi_N]$ wave with $v_{2\beta}$, $x_{0\mathrm{th}}=1.23$; and $a=-1$ for the $[\phi_N \to \pi]$ wave with $v_{3\beta}$, $x_{0\mathrm{th}}=1.16$, where $x_{0\mathrm{th}}=1/\lambda_{\mathrm{th}}$ [see Eq. (9)].

We note that, in this case, the absolute value of the asymptotic velocity corresponds to the *minimal* velocity, satisfying both the condition that the equilibrium ϕ_N is a node and the condition that the resulting profile is monotonic. Thus, the conclusion gained from the marginal stability theory, that the marginal value of velocity is realized asymptotically, is valid in this case also when the aforementioned additional restriction on monotonicity is taken into account.

For almost all solitary waves, listed in Table I, the wave width decreases with increasing absolute value of the asymptotic velocity, when the parameter a changes. Moreover, the product of $|v_i|$ and $w_{1/2}$ is seen to be approximately constant for a wide range of a values. This observation agrees with Eq. (9) because $w_{1/2}$ can be evaluated as $1/\lambda_{\mathrm{th}}$. The $[0 \to \pi]$ wave for $0<a<1/2$ does not satisfy this regularity, since both the wave velocity and the wave width decrease with increasing a.

We now discuss the possibility of applying our results to real cells. We can use formulas [Eqs. (12) and (13)] for v, if the cell thickness is much greater than the scale of the solitary wave, $d \gg 1/|\lambda_{\pm}|$. In this case the switching time can be evaluated as d/v_i. Possibly the most important result for applications is that the velocity of a wave having ϕ_N as one of the asymptotic states is greater than the velocity in other cases (see Fig. 3). Moreover, the velocities v_i, $i=1,2,3$, increase in absolute value with increasing magnitude of the electrical field $|E|$ (or, equivalently, increasing $|a|$). Therefore the switching time is seen to be essentially improved by choosing appropriate boundary conditions. The key idea is that one of the conditions should correspond to the lowest of the minima of the potential $V(\phi)$.

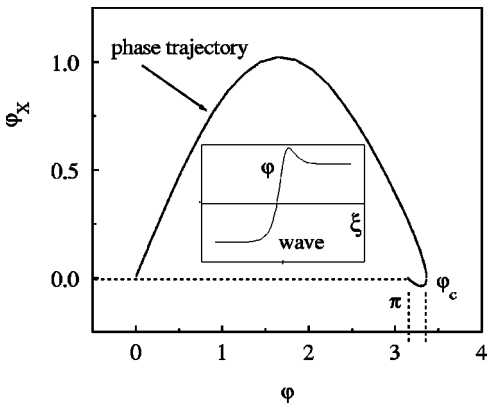

FIG. 5. Phase space of Eqs. (4),(11) for $a=0.4$ and $v=v_3=0.894$, calculated by using Eq. (12). The phase trajectory crosses the ϕ_X axis at the point $\phi=\phi_C$. The inset represents the solitary wave corresponding to this trajectory.

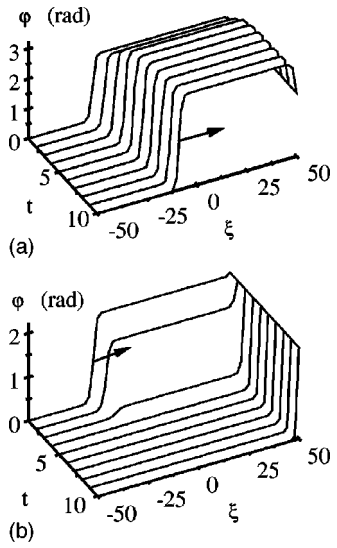

FIG. 6. Sensitivity to small variations of boundary conditions for a $[0 \to \phi_N]$ wave. (a) $\phi(50,t)=1.01\phi_N$; (b) $\phi(50,t)=0.99\phi_N$.

Another problem is the difficulty in preparing samples with exactly the required boundary conditions discussed above. The sensitivity to small variations of values at the boundaries for the $[0 \to \phi_N]$ wave is shown in Fig. 6. If the boundary value $\phi(+\infty,t)>\phi_N$ then the wave will transform to a $[0 \to \pi]$ wave, after which it will move with velocity v_4. If the boundary value $\phi(+\infty,t)<\phi_N$, then the value of ϕ near the right end of the interval decreases to 0; i.e. the switching will be faster than predicted. A solitary wave with an unstable state as one of the boundary conditions is physically an impossible object when considering *infinite* systems. However, similar structures can be realized in finite FLC cells. Suppose that the boundary condition on one cell plate corresponds to the stable state, while on the other plate the boundary condition represents an unstable state. With a switch of the electric field from zero to an appropriate value E_0, the solitary wave, which is a front from a stable to an unstable state, will propagate. We believe that the velocities of such waves in finite samples will be close to those velocities predicted by Eq. (12) for infinite systems. Probably, the switching speed could be optimized for sign reversing fields. Note that a change in the sign of E will give a different value of ϕ_N when $|a|>1/2$, so that one of the boundary values (ϕ_L or ϕ_R) will not be the static state. Therefore, the switch of E from E_0 to $-E_0$ will lead either to the breaking of the unstable state or to the propagation of several waves. Choosing appropriate values of system parameters and E_0, most likely, one could minimize the switching time. The results presented

here are novel and the consequences of reversing the field have yet to be exploited. Nevertheless, considering the single signed E field yielded some unexpected results, which are worthy of future investigation from both the theoretical and experimental points of view.

To evaluate the wave width and velocity we use the following values for the system parameters: $K\sim10^{-11}$ N, $P\sim10^{-5}$ C/m^2, $\eta\sim10^{-3}$ Pa c, $E\sim5\times10^{6}$ V/m. Then we have the space scale $x_0\sim0.4\times10^{-6}$ m and the time scale $t_0\sim2\times10^{-5}$ s, so that the characteristic velocity is $x_0/t_0=\sqrt{KPE}/\eta\sim0.02$ m/s. Therefore, for different values of E the wave velocity is of the order 10^{-2} to 10^{-1} m/s, while the width is $\sim0.5\times10^{-6}$ to 5×10^{-6} m. The assumption that $d\rightarrow\infty$ is correct for cells with thickness $d\sim10$ to 40 μm. The switching time in such cells is therefore of the order 10^{-5} to 10^{-3} s.

The results for solitary waves can be used in the analysis of the evolution of multikink profiles. Let us show this by considering the propagation of two solitary waves. Suppose that for some equilibrium state ϕ_m, the waves $[\phi_L-\phi_m]$ and $[\phi_m-\phi_R]$ exist. Let us then look for a solution to Eq. (2) in the form

$$\phi(\xi,\tau)=\phi^A(\xi,\tau)+\phi^B(\xi,\tau)-\phi_m, \tag{15}$$

which can be considered as the superposition of two solitary waves $[\phi_L-\phi_m]$ and $[\phi_m-\phi_R]$. Substituting Eq. (15) into Eq. (2), one can obtain a set of equations describing the ''interaction'' of solitary waves, labeled A and B:

$$\phi^A_\tau-\phi^A_{\xi\xi}+\sigma\cos(\phi^B-\phi_m)\sin\phi^A+a\{\cos[2(\phi^B-\phi_m)]\sin(2\phi^A)\}=0, \tag{16}$$

$$\phi^B_\tau-\phi^B_{\xi\xi}+\sigma\cos(\phi^A-\phi_m)\sin\phi^B+a\{\cos[2(\phi^A-\phi_m)]\sin(2\phi^B)\}=0. \tag{17}$$

Let us consider the wave A with the center (or extrema of ϕ^A_ξ) situated at $\xi=\xi^A$. If the distance $L\equiv\xi^B-\xi^A$ between the wave centers is large, the value $\epsilon\simeq1-\cos(\phi^B-\phi_m)$ in some neighborhood of the point ξ^A is small, $\epsilon\ll1$. Then the first equation (16) of the above set can be written as

$$\phi^A_\tau-\phi^A_{\xi\xi}+(1-\epsilon)\sigma\sin\phi^A+(1-4\epsilon)a\sin(2\phi^A)=0. \tag{18}$$

Assuming both ϕ^A and ϕ^B are ''sharp'' solitary waves, the parameter ϵ can be evaluated as $\epsilon=\delta\exp(-|v|L/2)$, where δ is some constant. Therefore the velocity of the A wave tends exponentially with increasing distance L to the velocity of the *single* $[\phi_L-\phi_m]$ wave.

The numerically calculated evolution of two kinks is shown in Fig. 7. The process of the interaction of $[0\rightarrow\phi_N]$ and $[\pi\rightarrow\phi_N]$ waves is demonstrated in Fig. 7(a). These waves move towards each other with velocities close to v_2, then they form a $[0\rightarrow\pi]$ wave, which propagates into the metastable state π with velocity v_4. Wave velocities obtained numerically are close to the velocities of single waves up to the point of wave annihilation. The splitting of a $[0\rightarrow\pi]$ wave to $[\phi_N\rightarrow0]$ and $[\phi\rightarrow\pi]$ waves is presented in Fig. 7(b). Notice that the evolutions displayed in Figs. 7(a) and 7(b) are realized for opposite signs of the electric field E, so that one can consider some of the stages in Fig. 7 as being representative of the evolution of ϕ after switching the direction of the field.

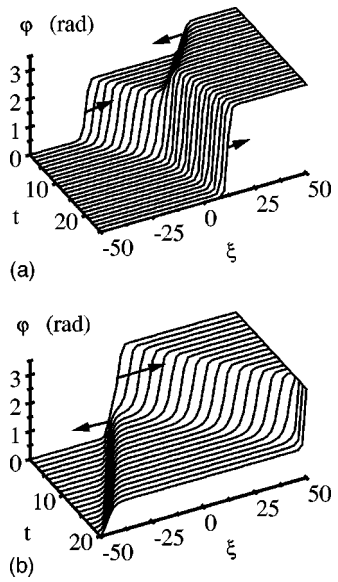

FIG. 7. Evolution of two-kink waves. (a) ''Annihilation'' of the $[0\rightarrow\phi_N]$ and $[\pi\rightarrow\phi_N]$ waves to the $[0\rightarrow\pi]$ wave, $a=1$; (b) the splitting of a $[0\rightarrow\pi]$ wave to the $[\phi_N\rightarrow0]$ and $[\phi_N\rightarrow\pi]$ waves, $a=-1$.

IV. CONCLUSIONS

In this paper a procedure for finding the parameters of solitary waves for nonlinear diffusion equations with appropriate boundary conditions is described. By using this procedure we have found parameters of solitary waves for smectic-C^* liquid crystals. We have shown that, by choosing appropriate boundary conditions, the resulting solitary waves have velocities greater than the velocity of a $[0-\pi]$ wave. This fact can be used for improving the switching time for electro-optical liquid crystal devices by optimizing the boundary conditions in finite cells to approximate those discussed above. For example, a cell designed to have ϕ_N as one of its boundary values can possess a faster switching time than that obtained via the usual $[0-\pi]$ wave; this has been discussed in detail in Sec. III above. The results, obtained for solitary waves in infinite systems, can therefore be exploited in the analysis of switching processes in finite systems and for studying the general evolution of multikink profiles.

ACKNOWLEDGMENTS

E.N.T. wishes to acknowledge the Royal Society/NATO Postdoctoral Fellowship Program for partial financial support of this work and the Department of Mathematics and Statistics, Edinburgh University, for its warm hospitality.

[1] P. G. de Gennes and J. Prost, *The Physics of Liquid Crystals* (Clarendon Press, Oxford, 1993).
[2] *Solitons in Liquid Crystals*, edited by L. Lam and J. Prost (Springer-Verlag, New York, 1992).
[3] L. Lam, Chaos Solitons Fractals **5**, 2463 (1995).
[4] M. C. Cross and P. C. Hohenberg, Rev. Mod. Phys. **65**, 851 (1993).
[5] P. E. Cladis, H. R. Brand, and P. L. Finn, Phys. Rev. A **28**, 512 (1983).
[6] J. E. Maclennan, M. A. Handschy, and N. A. Clark, Phys. Rev. A **34**, 3554 (1986).
[7] J. E. Maclennan, N. A. Clark, and M. A. Handschy, in *Solitons in Liquid Crystals* (Ref. [2]), pp. 151–190.
[8] I. Abdulhalim, G. Moddel, and N. A. Clark, J. Appl. Phys. **76**, 820 (1994).
[9] W. van Saarloos, M. van Hecke, and R. Holyst, Phys. Rev. E **52**, 1773 (1995).
[10] N. A. Clark and S. T. Lagerwall, Appl. Phys. Lett. **36**, 899 (1980).
[11] P. E. Cladis and W. van Saarloos, in *Solitons in Liquid Crystals* (Ref. [2]), pp. 110–150.
[12] F. M. Leslie, I. W. Stewart, and M. Nakagawa, Mol. Cryst. Liq. Cryst. **198**, 443 (1991).
[13] F. M. Leslie, I. W. Stewart, T. Carlsson, and M. Nakagawa, Continuum Mech. Thermodyn. **3**, 237 (1991).
[14] P. Schiller, G. Pelzl, and D. Demus, Liq. Cryst. **2**, 21 (1987).
[15] I. W. Stewart, T. Carlsson, and F. M. Leslie, Phys. Rev. E **49**, 2130 (1994).
[16] D. G. Aronson and H. F. Weinberger, Adv. Math. **30**, 33 (1978).
[17] V. A. Vasil'ev, Yu. M. Romanovskii, and V. G. Yakhno, *Avtovolnovye protsessy* (autowave processes) (Moscow, Nauka, 1987) (in Russian).
[18] P. S. Hagan, SIAM (Soc. Ind. Appl. Math.) J. Math. Anal. **13**, 717 (1982).
[19] E. Ben-Jacob, H. R. Brand, G. Dee, L. Kramer, and J.S. Langer, Physica D **14**, 348 (1985).
[20] W. van Saarloos, Phys. Rev. A **37**, 211 (1988).
[21] I. W. Stewart, IMA J. Appl. Math. **61**, 47 (1998).
[22] I. W. Stewart, Phys. Rev. E **57**, 5626 (1998).
[23] W. H. Press, B. P. Flannery, S. A. Teukolsky and W. T. Vetterling, *Numerical Recipes* (Cambridge University Press, Cambridge, 1986).